

1 **Past human expansions shaped the spatial pattern of Neanderthal ancestry**

2 Claudio S. Quilodrán^{1,2†}, Jérémy Rio^{1†}, Alexandros Tsoupas¹, Mathias Currat^{1,3*}

3

4 ¹ Department of Genetics and Evolution, University of Geneva, Switzerland

5 ² Department of Biology, University of Fribourg, Switzerland

6 ³ Institute of Genetics and Genomics in Geneva (IGE3), University of Geneva, Switzerland

7 † contributed equally to this work

8 * corresponding author: mathias.currat@unige.ch

9

10 **Summary**

11 The worldwide expansion of modern humans (*Homo sapiens*) from Africa started before the
12 extinction of Neanderthals (*Homo neanderthalensis*). Both species coexisted and interbred, as
13 revealed by the sequencing of Neanderthal genomes, leading to ~2% Neanderthal DNA in
14 modern Eurasians^{1,2}, with slightly higher introgression in East Asians than in Europeans³⁻⁶.
15 These distinct levels of ancestry have been argued to result from selection processes^{7,8}.
16 However, recent theoretical simulations have shown that range expansions could be another
17 explanation^{9,10}. This hypothesis would lead to the generation of spatial gradients of
18 introgression, increasing with the distance from the source of the expansion, i.e., Africa for
19 modern humans. Here, we investigate the presence of Neanderthal introgression gradients
20 after past human expansions by analysing an extended palaeogenomic dataset of Eurasian
21 populations. Our results show that the Out-of-Africa expansion of modern humans into
22 Eurasia resulted in spatial gradients of Neanderthal ancestry that persisted through time.
23 Moreover, while keeping the same gradient orientation, the expansion of early Neolithic
24 farmers into western Eurasia contributed decisively to reducing the average level of
25 Neanderthal genomic introgression in European compared to Asian populations. This is
26 because Neolithic farmers carried less Neanderthal DNA than preceding Palaeolithic hunter-
27 gatherers. This study shows that inferences about past population dynamics within our
28 species can be made from the spatiotemporal variation in archaic introgression.

29

30 **Keywords:** Population expansion, Admixture, Paleogenomics, Evolutionary dynamics,
31 Introgression, Neanderthal ancestry.

32

33 **Introduction**

34 Sequencing of Neanderthal genomes has revealed that ~2% of the DNA of modern humans
35 (MHs) outside of Africa is more similar to DNA from Neanderthals (NEs) than it is to DNA

36 from sub-Saharan populations^{1,2}. Two main, nonexclusive hypotheses have been proposed to
37 explain this pattern: (i) hybridization between NEs and MHs during their expansion out of
38 Africa (OOA), leading to the introgression of Neanderthal DNA segments into modern
39 humans^{1,2}; and (ii) incomplete lineage sorting resulting from ancestral population structure in
40 Africa, with ancestors of non-Africans more closely related to NEs than to sub-Saharan
41 Africans¹¹. Evidence in favour of hybridization has accumulated during the last decade^{5,12,13}.
42 However, the number, timing, and locations of interbreeding events between MH and NE
43 remain unclear. While early studies have suggested a single hybridization pulse in the Middle
44 East^{1,2}, a growing body of research supports the hypothesis of multiple hybridization
45 events^{6,10,14-16}. In particular, it has been shown that multiple hybridisation events over time
46 and space in western Eurasia are consistent with the levels of Neanderthal ancestry observed
47 in modern populations.¹⁰

48 While NE ancestry is relatively uniform among modern Eurasian populations^{1,2}, it is
49 approximately 8-24% higher in East Asia than in Europe³⁻⁶. This observation is surprising
50 since the known distribution of NEs was almost exclusively in the western part of Eurasia¹⁷.
51 Three major hypotheses have been proposed to explain the difference in NE ancestry between
52 western and eastern Eurasian populations: (i) higher effective population size in Europeans
53 compared to Asians, which led to a stronger effect of purifying selection acting on deleterious
54 NE alleles in the former⁷; (ii) dilution of NE ancestry in Europeans due to an input from a
55 hypothetical basal or “ghost” population with little or no NE ancestry^{18,19}; and (iii) multiple
56 pulses of NE introgression, where the original Eurasian introgression pulse was
57 supplemented by additional pulses after the divergence between the European and Asian
58 populations, resulting in different NE ancestry levels^{6,8,15,19}.

59 Recently, an additional hypothesis has been proposed, where different levels of NE
60 ancestry between western Europe and Eastern Asia are the result of the range expansion of
61 MHs after the OOA event⁹. Population range expansions have important evolutionary
62 consequences, including (i) creating gradients of allele frequencies^{20,21}; (ii) increasing the
63 frequency of specific alleles, whether neutral^{22,23} or under natural selection^{24,25}; (iii)
64 decreasing genetic diversity along the axis of expansion^{26,27}; and (iv) increasing mutational
65 load in populations through the maintenance of deleterious alleles²⁸. In addition, when
66 admixture with a local population occurs, population expansions tend to disproportionately
67 increase the genetic contribution of the local population to the invasive genetic pool, even if
68 interbreeding is limited²⁹. This latter effect is expected to result in the formation of spatial
69 gradients of neutral introgression along the axis of the biological invasions with hybridization

70 (see Fig. 1A). Under this assumption, introgression of local genes (i.e., NEs) increases in the
71 invasive population (i.e., MHs) with the distance from the source of the expansion (i.e.,
72 Africa). This is due to the combined effects of i) demographic imbalance between the
73 expanding population and the local population at demographic equilibrium, ii) continuous
74 hybridization events at the wave front of the range expansion, and iii) genetic surfing. This
75 hypothesis could therefore explain different levels of Neanderthal ancestry in Europe and
76 East Asia by differences in geographical distance from the source of the MH expansion in
77 Africa⁹. Quilodrán, et al. ⁹ showed that the process of range expansion could explain the
78 difference in NE ancestry between Europe and East Asia using computational simulations
79 based on a limited amount of genomic information from the two extreme sides of the
80 continent (West and East). However, neither a detailed inspection of geographic introgression
81 patterns (i.e., the existence of gradients) nor their change over time was included in this
82 preliminary study. Indeed, range expansions occurred not only during the OOA expansion¹⁰
83 but also during other prehistoric periods³⁰. This includes the European Neolithic transition,
84 when farmers coming from southeast Europe partially replaced hunter-gatherers³¹⁻³⁴, as well
85 as the Bronze Age, with the spread of pastoralist populations from Eurasian steppes³⁵⁻³⁷.
86 Therefore, multiple population movements during recent human history could have
87 contributed to shaping NE ancestry across time and space because distinct expanding
88 populations can carry various levels of NE ancestry^{20,30,38}.

89 Here, we investigate whether spatial gradients of introgression consistent with the
90 range expansion hypothesis have occurred in Eurasia by examining the levels of NE ancestry
91 in human populations distributed across space and time. Our study demonstrates that
92 spatiotemporal levels of introgression provide valuable information about past population
93 dynamics, suggesting multiple episodes of range expansion as a main force shaping archaic
94 introgression levels during human evolutionary history.

95 96 **Results and discussion**

97 *Spatial gradients of Neanderthal ancestry in Eurasia*

98 We analysed an extended dataset of 4464 published ancient and modern genomes (from
99 ~40000 years BP to present time) retrieved from the Allen Ancient DNA database³⁹. We
100 associated each genome with one of the following population groups: Palaeolithic/Mesolithic
101 hunter-gatherers (HGs), Neolithic Chalcolithic farmers (FAs), other ancient samples (OTs) or
102 modern samples (MDs). We estimated NE introgression for all genomes and averaged the
103 introgression estimates for genomes from the same geographic coordinates, time periods and

104 population group, leading to $n = 2625$ samples (Fig. 1B). We then explored the fixed effect of
105 latitude, longitude, time (dates in years BP), continental area (Europe or Asia), and their
106 interactions by using a linear mixed model (LMM) with log-transformed NE ancestry as the
107 response variable. LMMs are particularly useful for dealing with hierarchical structures and
108 the nonindependence of the dataset. We investigated the random effect of the population
109 group, the period nested within these groups (in clusters of 500 years), and the spatial and
110 temporal autocorrelation of data. This model was called “Full Eurasia” because it uses the
111 whole palaeogenomic dataset. Based on the lowest AIC value⁴⁰, the best LMM was retained
112 (Table S1, supporting information).

113 By considering the average date of all samples as a time reference (~4200 years BP),
114 we observed a linear relationship of NE ancestry with latitude and longitude, both in Europe
115 and Asia (Fig. 2, Table S1). These geographic patterns support the hypothesis of spatial
116 introgression gradients generated after population expansion with hybridization¹⁰,
117 schematically represented in Fig. 1A, in which the introgression of local genes (i.e., NEs) is
118 expected to increase in the invasive population (i.e., MHs) with the distance from the source
119 of its expansion (i.e., Africa). While a positive relationship with latitude is observed in
120 Europe and Asia (Fig. 2A), a contrasting relationship is observed with longitude, positive in
121 Asia and negative in Europe (Fig. 2B). The increasing NE introgression with latitude is
122 compatible with the OOA expansion of MHs from southern to northern areas of Eurasia
123 while hybridizing with NEs. The longitudinal pattern is compatible with a source of
124 expansion in the Middle East, from which NE ancestry is expected to increase with longitude
125 in Asia but decrease with longitude in Europe. Although alternative evolutionary forces may
126 also be responsible for creating introgression gradients (e.g., spatially varying selective
127 pressure), the specific pattern we observed with a source of all spatial gradients in the Middle
128 East makes population range expansion the most parsimonious explanation.

129 Alternatively, spatial variation of NE ancestry in MH could result from an unequal
130 distribution of NEs in Eurasia, with more interspecific interactions occurring in areas where
131 NE were more numerous, resulting in more local admixture. We find a higher NE ancestry
132 level in Europe than in Asia after the OOA (Fig. 3), which is in accordance with the current
133 fossil record of NEs in Eurasia, with more accumulated evidence in Europe. Moreover, our
134 results showing more NE ancestry in northern Eurasia than in southern Eurasia further concur
135 with evidence of NE presence in the northern Himalayas¹⁷, even if an undetected presence in
136 the south cannot be ruled out. Nevertheless, even in the case of unequal distribution of the
137 local species, increasing gradients of introgression in the invasive population (i.e., MHs)

138 resulting from range expansion may remain a valid explanation. For instance, this is expected
139 after a range expansion where the local population is only occupying a part of the area⁹, as
140 was probably the case for NEs in Eurasia.

141 However, our analysis does not support the hypothesis that a slightly higher level of
142 NE ancestry in East Asia than in Western Europe today could be explained by the greater
143 distance to the source of the MH expansion in Asia than in Europe⁹. This hypothesis was
144 made from modern DNA data only, while our results also considered ancient DNA samples.
145 Using palaeogenomic data, we show the reverse pattern for samples older than 20000 years
146 BP, with more NE ancestry observed in Europe than in Asia (Fig. 3). The current pattern of
147 NE ancestry being higher in Asia than in Europe must thus have developed at a later stage.

148

149 *Temporal variation in Neanderthal ancestry*

150 Our results suggest that the longitudinal gradient slope has remained similar over the last
151 40000 years (Table S1, supporting information), whereas the latitudinal gradient of NE
152 ancestry has significantly changed over time ($F = 4.4$, $P = 0.03$). The latitudinal pattern is
153 more prominent during the early period in Europe and becomes less visible ~30000 years BP,
154 together with an overall reduction in NE ancestry (Fig. 3). While this implies that the level of
155 NE ancestry in Eurasia may not have been uniformly distributed across space as is observed
156 today, this expectation needs to be confirmed with more palaeogenomes because the
157 interaction between latitude and time is no longer significant when considering the average of
158 all candidate models (based on a cumulative weighted AIC of 90%, $\sum \omega_i \geq 0.90$, Table S2,
159 supporting information) instead of the best model only.

160 The variation in NE ancestry across time is currently debated. It has been proposed
161 that ancient European genomes showed more NE ancestry compared to present-day
162 Europeans¹², but this result was questioned because of a methodological bias in the ancestry
163 estimation procedure⁴¹. Nevertheless, it has been estimated that NE ancestry could have been
164 as high as 10% at the time of admixture before decreasing rapidly to the current rate of
165 ~2%⁴². Here, we show that the temporal reduction in NE ancestry is linked to latitude. The
166 southern samples in Europe show an almost constant NE ancestry through time, while the
167 northern samples experienced a reduction between approximately 40000 and 20000 years BP.
168 The latitudinal gradient could have undergone important changes, possibly due to population
169 expansions and contractions experienced by MHs during the Last Glacial Maximum (LGM)
170 or other, more limited ice ages. Our results show that this gradient becomes less evident in

171 modern data (Fig. 3). Because the longitudinal pattern has been less affected during the last
172 40000 years, it may represent a relict signature of the OOA range expansion that occurred
173 during MH evolution between 60000 and 45000 years BP.

174 Natural selection has been invoked to explain the reduction in NE ancestry over
175 time^{7,43}, but different historical processes could have also played an important role. This
176 includes population expansions and contractions^{44,45}, as well as interactions between
177 genetically differentiated populations with different levels of NE ancestry^{18,19}. In Europe, a
178 prominent genetic transition occurred during the spread of early Neolithic farmers, when they
179 partially replaced Palaeolithic/Mesolithic hunter-gatherers (e.g. the so-called Neolithic
180 transition)^{31,32-34}. This transition began in the Fertile Crescent ~11000 years BP⁴⁶, and its
181 consequences on the distribution of NE ancestry have been weakly explored thus far¹⁸.

182

183 *Early farmers carried less Neanderthal ancestry than hunter-gatherers in Europe*

184 We thus explored more specifically the variation in the level of NE ancestry across time and
185 population groups (HGs, FAs, OTs, $n = 2534$ in total). The OT group includes all ancient
186 samples that are neither FAs nor HGs, including for example, the Bronze Age and more
187 recent periods. Samples from the MD group were excluded from this analysis because they
188 do not allow us to explore temporal variation in NE ancestry (all modern data are associated
189 with the same date). We included population groups, continental area (either Europe or Asia),
190 time and their interactions as fixed variables, also correcting for spatial autocorrelation in the
191 dataset. This model is called “Ancient Eurasia” because it only considers ancient samples and
192 its best LMM is presented in Table S1 (supporting information). We observed an influence of
193 time on the differences between Europe and Asia ($F = 9.22$, $P < 0.01$) and population groups
194 ($F = 9.41$, $P < 0.01$), with an overall higher NE ancestry level for HGs than for FAs,
195 particularly visible in Europe (Fig. 4). At approximately 10000 years BP, when the first FA
196 appeared in the Near East, the difference between FAs and HGs was significant in Europe
197 (HG: 0.024 ± 0.001 (estimated mean \pm se), FA: 0.019 ± 0.001 , t ratio = -6.14 , $P < 0.001$), as
198 well as in Asia (HG: 0.022 ± 0.001 , FA: 0.018 ± 0.001 , t ratio = -6.14 , $P < 0.001$).

199 Approximately 6000 years BP, when farming was well established but some HG populations
200 persisted, the difference in NE ancestry was still significant between the HG (0.023 ± 0.001)
201 and FA (0.020 ± 0.0002) populations in Europe (t ratio = -4.21 , $P < 0.001$), as well as
202 between the HG and OT (0.020 ± 0.0003) populations (t ratio = 3.51 , $P = 0.001$), but not
203 between the FA and OT populations (t ratio = -0.41 , $P = 0.91$). A similar situation was
204 observed in Asia at this time (FAs vs. HGs, t ratio = -4.26 , $P < 0.001$; HGs vs. OTs, t ratio =

205 3.51, $P = 0.001$; FAs vs. OTs, t ratio = -0.41, $P = 0.91$). Overall, this means that earlier FA
206 carried less NE ancestry than the former HGs of the same area. This difference vanished over
207 time, since the level of NE ancestry in FAs increased during the cohabitation period with
208 HGs in both geographic regions (Fig. 4). While Asian FAs reached an average level similar
209 to that of HGs, European FAs did not reach such a high level (Fig. 4). Thus, FAs could have
210 acted as a population that diluted NE ancestry in Western Eurasia, as previously
211 suggested^{18,19}.

212 Multiple episodes of range expansion of populations where levels of NE ancestry
213 differed could provide an explanation for the spatiotemporal change in NE ancestry. Our
214 results support our former expectation that human past range expansions (i.e., HGs then FAs)
215 contributed to the creation of spatial gradients of NE ancestry, with the level increasing from
216 their source in Southwest Asia (Fig. 2 and Fig. 3). The second range expansion into Western
217 Eurasia, that of early FAs with a lower level of NE ancestry, is critical to explain the overall
218 dilution of NE ancestry in this area. The later expansion of the steppe pastoralists does not
219 seem to have had as much influence as there is not a significant difference between the FA
220 and OT population groups, but this would require a more detailed examination, as our OT
221 group includes populations from different cultural periods.

222

223 *Spatial gradients in European farmers and hunter-gatherers*

224 We then decided to focus our analysis on Europe due to the larger density and more uniform
225 distribution of palaeogenomes than in Asia, where the Palaeolithic and Neolithic eras are
226 represented by a lower number of samples that cover a larger area (1517 samples in Europe
227 vs. 1108 samples in Asia for an area four times as large, Fig. 1B). Moreover, domesticated
228 plants and animals occurred in more than one site in Asia^{47,48}, making exploration of past FA
229 population dynamics more challenging than in Europe.

230 By using a subsample of data restricted to Europe ($n = 1517$), we explored the effect
231 of latitude, longitude, and population groups (HG-FA-OT-MD) on NE ancestry, controlling
232 for the fixed effect of time. We excluded cross-level interactions between time and
233 population groups because of the lack of temporal variation in MD samples. The LMM is
234 called “Europe” and its best version is presented in Table S1 (supporting information). The
235 interaction between longitude and population group was nonsignificant and excluded during
236 model selection, together with the interaction between latitude and population groups (Table
237 S1 and Table S2). This implies that the negative longitudinal trend and positive latitudinal
238 trend shown in Figure 2 remain for all population groups in Europe, despite the higher NE

239 ancestry in HGs compared to other cultural populations (Fig. 5). The interaction between
240 latitude and longitude was significant ($F = 29.29$, $P < 0.001$), meaning that their introgression
241 slopes were interdependent for all population groups (Fig. 5 and Fig. S1, supporting
242 information). When considering the full model that includes all fixed variable interactions,
243 the only spatial gradient that has changed is the slope of latitude for HGs compared to FAs (F
244 $= 2.68$, $P = 0.04$, Table S3, supporting information). Although the result for HGs may be
245 influenced by the scarcity of samples during the Palaeolithic, this analysis suggests that the
246 latitudinal variation could have changed more than the longitudinal variation during this
247 period (Fig. 3 and Fig. 5). Different events of population contractions and expansions during
248 the Palaeolithic related to the LGM^{44,45} could have affected the latitudinal gradient more than
249 the one seen for longitude. Overall, the spatial trend remains similar across different periods
250 of time, becoming less pronounced in modern samples (Fig. S1, supporting information) and
251 with a higher NE ancestry in HGs (Fig. 5).

252 In Europe, both the early human expansion during the Palaeolithic and the farming
253 expansion during the Neolithic trace back to Southwest Asia³⁰, where we estimated the
254 lowest level of NE ancestry. The difference in NE ancestry between HGs in Europe and in
255 Anatolia, where FAs originated (see red area and blue area for HGs, respectively, Fig. 5),
256 explains why early FAs contributed to an overall reduction in the level of NE ancestry when
257 expanding across Europe (Fig. 5). Note that it was recently found that modern Levantine and
258 southern Arabian populations still have lower NE ancestry than northern Eurasian
259 populations⁴⁹.

260 According to the expansion hypothesis⁹, as HGs spread over Europe, their NE
261 introgression levels increased due to a combination of stochastic demographic and migratory
262 processes related to gene surfing^{22,23} and gene dilution^{20,30,38}, which explains the spatial
263 gradients of NE ancestry observed in HGs (Fig. 5). Later, a second expansion occurred
264 during the Neolithic, following approximately the same direction as the expansion of HGs.
265 Consequently, the spatial gradient already present in HGs was maintained in FAs because
266 both populations admixed (Fig. 5). As previously noted⁴⁴, the sole observation of a South
267 East to North West genetic cline in Europe is not informative about the expansion of FAs, as
268 the cline could have been generated during the previous HG expansion. Here, our results
269 suggest that the NE ancestry cline was produced during the HG range expansion and was
270 affected by the later expansion of FAs during the Neolithic transition while maintaining the
271 same general orientation. As FAs had initially less NE ancestry than HGs, it lowered the
272 average amount in the admixed European population. This corresponds to the model of

273 population expansion with partial replacement supported by palaeogenomic studies for the
274 Neolithic³¹⁻³³. In the absence of admixture between HGs and FAs, we would have expected a
275 larger decrease in NE ancestry in FA populations, whereas with a large admixture, the
276 gradients in FAs would have rapidly reached that of HGs in Europe.

277

278 *Conclusion*

279 Our findings highlight the evolutionary impact of past range expansions in generating spatial
280 gradients of NE ancestry in MHs. We observed that these ancestry levels were more spatially
281 heterogeneous in the past and that they became more homogeneous during the Holocene
282 under the effect of gene flow resulting from population movements and migrations. Complex
283 population movements and genetic interactions are reflected when analysing the level of NE
284 ancestry in different regions (Europe and Asia) and in populations with different cultural
285 backgrounds (hunter-gatherers and farmers). The spatial gradient of NE ancestry in HGs is
286 compatible with a model of range expansion of MHs during the OOA expansion. After this
287 first expansion, the level of NE ancestry was slightly higher in western Eurasia than in
288 eastern Eurasia. Then, a second range expansion of early FAs with a lower NE ancestry than
289 HGs occurred in Europe during the Neolithic transition, from the southeast towards the
290 northwest. This second range expansion is essential for explaining the pattern currently
291 observed of lower NE ancestry in Western Europe than in East Asia³⁻⁶. Our results therefore
292 do not support our previous hypothesis that the slightly greater NE ancestry in Eastern
293 Eurasia compared to Western Eurasia is due to population dynamics during the OOA
294 expansion of MHs taking place ~ 40000 BP. Instead, our results reveal that the current
295 geographical heterogeneity of NE ancestry is due to dynamics that occurred during the more
296 recent Neolithic expansion ~10,000 BP. The early FA populations, which are probably
297 related to the previously identified basal Eurasian lineage^{18,19,49}, admixed with HG, leading to
298 a progressive increase in HG ancestry and consequently NE ancestry in the expanding FA
299 populations. The partial replacement of HGs by FAs^{31,32} thus contributed to reducing the
300 level of NE ancestry in western Eurasia more than in eastern Eurasia. While selection was
301 invoked to explain the difference between Europe and Asia⁴³, the neutral hypothesis of
302 historical range expansions is sufficient to explain past and current patterns of NE ancestry in
303 humans.

304 Although the introgression of archaic material in MHs was probably counterselected
305 during an initial stage⁴¹, the fact that the amount of NE introgression is relatively stable
306 through time, approximately 2%, suggests that this remaining small portion of introgressed

307 DNA can be considered to evolve generally neutrally. This assumption is also supported by
308 the observation that archaic introgression tends to be rarer in gene-rich regions⁷. However,
309 there are exceptions to this general pattern, with examples of adaptive introgression related to
310 the immune system^{50,51}, skin pigmentation¹⁵ and altitude⁵², providing a better adaptation to
311 local environmental conditions and pathogens⁵³. Moreover, in present-day populations, some
312 loci introgressed from archaic hominins appear to influence disease risk, such as
313 neurological, psychiatric, immunological, dermatological and dietary disorders^{5,54}, either
314 positively or negatively. It is thus crucial to describe neutral patterns of introgression
315 resulting from human demography and migration to allow better detection of loci under
316 selection (positive or negative) as outliers of the neutral background. It could help to
317 reconstruct the impact of past epidemics on the evolution of human immunity. Additional
318 palaeogenomic data for the most ancient periods combined with alternative modelling
319 methods should allow a more detailed understanding of evolutionary processes leading to
320 similar diversity patterns. These developments would provide a better understanding of both
321 the population dynamics within our species and its interactions with other extinct archaic
322 species, such as Neanderthals and Denisovans.

323

324 **Material and Methods**

325 **Dataset**

326 Palaeogenomic data available for Eurasian populations were retrieved from the AADR
327 database (Allen Ancient DNA Resource v50.0³⁹). This database includes 10391 genomes. For
328 each genome, we retained the mean date in years before present (BP) reported in the
329 database, which corresponds either to the mean of the 95.4% CI calibrated radiocarbon age or
330 to the mean of the archaeological context range. We only included genomes from individuals
331 located in Eurasia in our analysis, with longitude 34° as a delimiter, i.e., west of 34° is
332 considered Europe in our analyses, while east of 34° is considered Asia. For genomes that
333 have multiple versions in the database, we retained for analysis only the version with the
334 most SNPs. We filtered out putatively contaminated palaeogenomes by using the
335 contamination warning estimated through linkage disequilibrium⁵⁵ (values of
336 “*contamLD_warning*” being either “*Model_Misspecified*” or “*Very_High_Contamination*”
337 were removed) as well as by excluding genomes that contained “contam” or
338 “possible.contam” in their GroupID name. Moreover, we excluded from the downstream
339 analysis all the genomes missing the geographical coordinates of the location of their origin
340 or information about the population group to which they belong.

341 We assigned each genome to a population group based either on the information
342 provided by the GroupID parameter or on the information provided in the publications that
343 produced these genomes: Palaeolithic and Mesolithic hunter-gatherers (HG, $n=135$),
344 Neolithic and Chalcolithic farmers (FAs, $n=810$), other ancient genomes not belonging to HG
345 and FA (OT, $n=2327$), and modern genomes (MDs, $n=1192$), which are referenced by a date
346 zero in the database. The table S4 in supporting information lists all the genomes used in our
347 analysis.

348

349 **Estimation of Neanderthal ancestry**

350 We used F4-ratios as introduced by Reich et al.⁵⁶ to estimate NE ancestry (α) in each genome
351 of interest. It is calculated as the ratio of two F4-statistics generated from five populations,
352 where one population results from the admixture between two others. We followed Petr et al.
353 ⁵⁵ to avoid a bias in the temporal distribution of the F4-statistics. This procedure considers the
354 reflux of NE introgression from European populations into northern and western African
355 populations using the Dinka population from eastern Africa as a sister population (“C”) of the
356 tested genome (“X”) instead of the Yoruba from western Africa. The Altai Neanderthal (“A”)
357 was used as a sister population of the Vindija Neanderthal (“B”), and chimpanzee was
358 included as an outgroup (“O”). The value of α estimates the proportion of ancestry deriving
359 from B in an admixed genome X, using the same A, C and O populations as references: $\alpha =$
360 $F4(A, O, X, C)/F4(A, O, B, C)$, where X = test genome; A = Altai_Neanderthal. DG; B =
361 Vindija_Neanderthal. DG; C = Dinka. DG; O = Chimp. REF; all retrieved from the AADR
362 database. We refer to this observed F4 ratio as Neanderthal ancestry (or introgression).

363 We used the R package ADMIXTOOLS 2 to compute the F4-ratio for each genome⁵⁷.

364 Only genomes showing a significant value ($Z > 3$) were included in our analyses to ensure
365 the accuracy of the estimated NE ancestry. This resulted in 4464 genomes. The European
366 area is represented by 2146 palaeogenomes, and the Asian area is represented by 2318
367 palaeogenomes. We averaged the F4-ratio for genomes with the same date, geographic
368 coordinates and population group, resulting in a final dataset of 2625 population samples
369 (from ~40000 years BP to modern time, 1517 in Europe and 1108 in Asia, Fig. 1B).

370

371 **Statistical analysis**

372 We used the computed F4-ratio as the response variable in a series of linear mixed model
373 (LMM) analyses, which are especially well suited to describe the relation between variables,
374 including autocorrelation and missing data. This response variable was log-transformed to

375 maintain the Gaussian distribution of residuals. In the first analysis, we included latitude,
376 longitude, time (years BP), continental area (Europe or Asia), and their interactions as
377 explanatory (fixed) variables. We evaluated the effect of the population groups (HG, FA, OT
378 and MD), as well as the nested effect of time period within these population groups (i.e.,
379 grouping dates within 500 years ranges), as random variables. We also evaluated the
380 influence of the spatial autocorrelation and temporal autocorrelation of the dataset. The
381 choice of fixed and random model structures from among those investigated and the selection
382 of the best model was based on the lowest Akaike Information Criterion value (AIC)⁴⁰,
383 following Zuur et al.⁶⁷. The final model structure was an LMM that considered the period
384 nested in the population groups as a random intercept and slope of continental area, as well as
385 an exponential spatial autocorrelation. We called this model “Full Eurasia” because it
386 incorporates the whole dataset (Table S1, supporting information).

387 Because the ancient DNA samples belonging to different population groups were not
388 equally distributed throughout Europe and Asia, we ran two additional LMM analyses using
389 subsets of the data to explore in more detail the fixed effect of population groups on the log-
390 transformed F4-ratio. The autocorrelation structure, as well as the random and fixed effects of
391 both models, were selected in a similar way as the “Full Eurasia” model. First, we focused on
392 the temporal trend in Europe and Asia, considering time, continental area, and population
393 groups (HG-FA-OT) as fixed variables, also including their respective interactions in the
394 model. We excluded MD samples because there is no variation allowing a cross-level
395 interaction with time (all dates are identical). The final model structure considered the period
396 (i.e., in clusters of 500 years) as a random intercept and slope of continental area, as well as
397 an exponential spatial autocorrelation. This model is reported as “Ancient Eurasia” because it
398 considers only the ancient genomes from Eurasia as a whole (Table S1, supporting
399 information). Second, because the spatial density of available palaeogenomes (i.e., the
400 number of palaeogenomes per millions of square kilometres) is much larger in Europe
401 (191.55) than in Asia (28.15), we focused the spatial analysis of population groups on
402 Europe. The fixed variables were latitude, longitude, population groups (HG-FA-OT-MD)
403 and their interactions, also including time as a fixed covariate. The interaction between time
404 and population groups was excluded because of the lack of temporal variation in MD
405 samples. The final LMM considered the period as a random intercept, as well as a ratio
406 quadratic spatial autocorrelation. This model is reported as “Europe” (Table S1, supporting
407 information).

408 For all three LMM analyses, we verified collinearity among fixed variables by
409 computing the variance inflator factor (VIF). All variables included in the separate models
410 did not show collinearity with other variables ($VIFs < 4$)⁵⁸. We reported the conditional
411 ($R^2_{GLMM(c)}$) and marginal ($R^2_{GLMM(m)}$) coefficients of determination for the selected LMMs
412 (Table S5, supporting information). They denote the proportion of variance explained by
413 fixed variables and both fixed and random variables, respectively⁵⁹. Because the number of
414 samples within continental locations and groups of populations were not the same, we
415 reported mean differences by considering an ANCOVA with sum of squares of type III. A
416 Tukey correction was implemented for multiple post hoc comparisons among population
417 groups. We reported trends of continuous variables by considering the average values of
418 other predictors within continental areas and population groups (Table S6, supporting
419 information), except when it is specifically mentioned in the main text. We show the outputs
420 of the best models after the selection of the random and fixed structure (Table S1, supporting
421 information), but we also show the average of candidate models based on a cumulative
422 weighted AIC of 90% ($\sum \omega_i \geq 0.90$, Table S2, supporting information), as well as the full
423 model without selection of fixed variables (Table S3, supporting information). The last two
424 models were referred to when a nonsignificant relationship was excluded from the best
425 models. All analyses were carried out using the R language⁷⁰. The *nlme* package⁷¹ was used
426 for the LMMs, the *emmeans* package⁷³ for multiple comparisons, and the *MuMIn* package⁷²
427 for the estimation of pseudodetermination coefficients and model averaging.

428

429 **Author contribution**

430 All authors contributed to the design of the study, the interpretation of the results and to the
431 writing of the manuscript. MC coordinated the study. JR and AT formatted the data. JR, CQ
432 and AT performed the analyses. JR and CQ drafted the manuscript.

433

434 **Acknowledgments**

435 This project was financially supported by the Swiss National Research Foundation grant
436 n° 31003A_182577 to MC and n° P5R5PB_203169 to CSQ. The authors would like to thank
437 Pascale Gerbault and Paola Cerrito and Lionel Di Santo for a careful reading of the
438 manuscript.

439

440 **Data availability statement**

441 All the data analysed were previously published and retrieved from the Allen Ancient DNA
442 Resource v50.0 ([https://reich.hms.harvard.edu/allen-ancient-dna-resource-aadr-](https://reich.hms.harvard.edu/allen-ancient-dna-resource-aadr-downloadable-genotypes-present-day-and-ancient-dna-data)
443 [downloadable-genotypes-present-day-and-ancient-dna-data](https://reich.hms.harvard.edu/allen-ancient-dna-resource-aadr-downloadable-genotypes-present-day-and-ancient-dna-data)). The table S4 in supporting
444 information lists all the genomes used in our analysis with their indexes in the AADR
445 database and their original references, as well as the associated population groups.

446

447 **Code availability**

448 All the R packages used to perform the analyses are listed in the Material and Method section
449 and freely available from the Comprehensive R Archive Network (<https://cran.r-project.org/>).

450

451 **Competing interests**

452 The authors declare no competing interests.

453

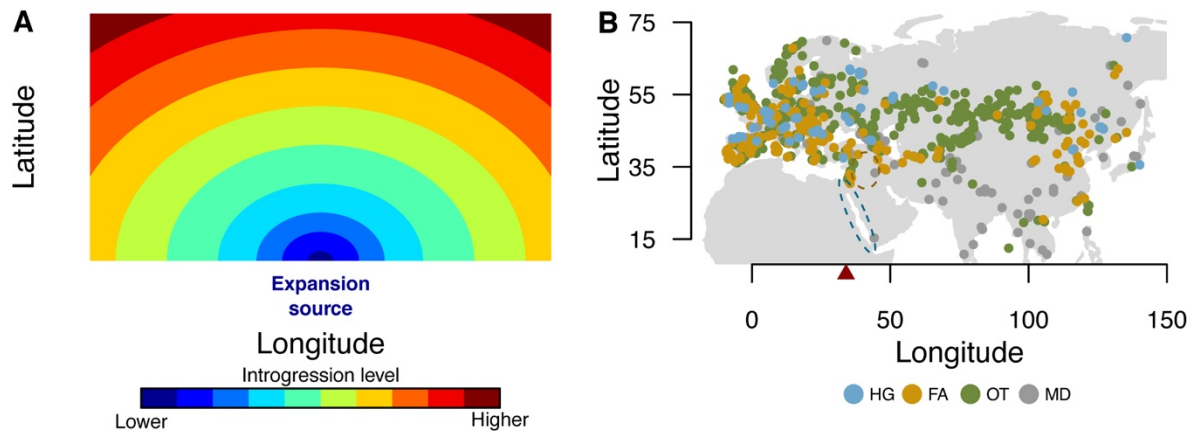
454 **References**

- 455 1 Green, R. E. *et al.* A draft sequence of the Neandertal genome. *Science* **328**, 710-722
456 (2010). [https://doi.org:10.1126/science.1188021](https://doi.org/10.1126/science.1188021)
- 457 2 Reich, D. *et al.* Genetic history of an archaic hominin group from Denisova Cave in
458 Siberia. *Nature* **468**, 1053-1060 (2010). [https://doi.org:10.1038/Nature09710](https://doi.org/10.1038/Nature09710)
- 459 3 Chen, L., Wolf, A. B., Fu, W., Li, L. & Akey, J. M. Identifying and Interpreting
460 Apparent Neanderthal Ancestry in African Individuals. *Cell* **180**, 677-687 e616
461 (2020). [https://doi.org:10.1016/j.cell.2020.01.012](https://doi.org/10.1016/j.cell.2020.01.012)
- 462 4 Meyer, M. *et al.* A high-coverage genome sequence from an archaic Denisovan
463 individual. *Science* **338**, 222-226 (2012). [https://doi.org:10.1126/science.1224344](https://doi.org/10.1126/science.1224344)
- 464 5 Prufer, K. *et al.* A high-coverage Neandertal genome from Vindija Cave in Croatia.
465 *Science* **358**, 655-658 (2017).
- 466 6 Wall, J. D. *et al.* Higher Levels of Neanderthal Ancestry in East Asians than in
467 Europeans. *Genetics* **194**, 199-+ (2013). [https://doi.org:10.1534/genetics.112.148213](https://doi.org/10.1534/genetics.112.148213)
- 468 7 Sankararaman, S. *et al.* The genomic landscape of Neanderthal ancestry in present-
469 day humans. *Nature* (2014). [https://doi.org:10.1038/nature12961](https://doi.org/10.1038/nature12961)
- 470 8 Villanea, F. A. & Schraiber, J. G. Multiple episodes of interbreeding between
471 Neanderthal and modern humans. *Nat Ecol Evol* **3**, 39-44 (2019).
472 [https://doi.org:10.1038/s41559-018-0735-8](https://doi.org/10.1038/s41559-018-0735-8)
- 473 9 Quilodrán, C. S., Tsoupas, A. & Currat, M. The Spatial Signature of Introgression
474 After a Biological Invasion With Hybridization. *Front Ecol Evol* **8** (2020).
475 [https://doi.org:10.3389/fevo.2020.569620](https://doi.org/10.3389/fevo.2020.569620)
- 476 10 Currat, M. & Excoffier, L. Strong reproductive isolation between humans and
477 Neanderthals inferred from observed patterns of introgression. *Proc Natl Acad Sci U*
478 *S A* **108**, 15129-15134 (2011). [https://doi.org:10.1073/pnas.1107450108](https://doi.org/10.1073/pnas.1107450108)
- 479 11 Eriksson, A. & Manica, A. Effect of ancient population structure on the degree of
480 polymorphism shared between modern human populations and ancient hominins.
481 *Proc Natl Acad Sci U S A* **109**, 13956-13960 (2012).
482 [https://doi.org:10.1073/pnas.1200567109](https://doi.org/10.1073/pnas.1200567109)

- 483 12 Fu, Q. M. *et al.* The genetic history of Ice Age Europe. *Nature* **534**, 200-+ (2016).
484 [https://doi.org:10.1038/nature17993](https://doi.org/10.1038/nature17993)
- 485 13 Racimo, F., Sankararaman, S., Nielsen, R. & Huerta-Sanchez, E. Evidence for archaic
486 adaptive introgression in humans. *Nat Rev Genet* **16**, 359-371 (2015).
487 [https://doi.org:10.1038/nrg3936](https://doi.org/10.1038/nrg3936)
- 488 14 Kuhlwilm, M. *et al.* Ancient gene flow from early modern humans into Eastern
489 Neanderthals. *Nature* **530**, 429-+ (2016). [https://doi.org:10.1038/nature16544](https://doi.org/10.1038/nature16544)
- 490 15 Vernot, B. & Akey, J. M. Resurrecting Surviving Neandertal Lineages from Modern
491 Human Genomes. *Science* **343**, 1017-1021 (2014).
492 [https://doi.org:10.1126/science.1245938](https://doi.org/10.1126/science.1245938)
- 493 16 Prufer, K. *et al.* The complete genome sequence of a Neanderthal from the Altai
494 Mountains. *Nature* **505**, 43-49 (2014). [https://doi.org:10.1038/nature12886](https://doi.org/10.1038/nature12886)
- 495 17 Krause, J. *et al.* Neanderthals in central Asia and Siberia. *Nature* **449**, 902-904
496 (2007). [https://doi.org:10.1038/nature06193](https://doi.org/10.1038/nature06193)
- 497 18 Lazaridis, I. *et al.* Genomic insights into the origin of farming in the ancient Near
498 East. *Nature* **536**, 419-+ (2016). [https://doi.org:10.1038/nature19310](https://doi.org/10.1038/nature19310)
- 499 19 Vernot, B. & Akey, J. M. Complex history of admixture between modern humans and
500 Neandertals. *American journal of human genetics* **96**, 448-453 (2015).
501 [https://doi.org:10.1016/j.ajhg.2015.01.006](https://doi.org/10.1016/j.ajhg.2015.01.006)
- 502 20 Barbujani, G., Sokal, R. R. & Oden, N. L. Indo-European origins: a computer-
503 simulation test of five hypotheses. *Am J Phys Anthropol* **96**, 109-132 (1995).
- 504 21 Rendine, S., Piazza, A. & Cavalli-Sforza, L. Simulation and separation by principal
505 components of multiple demic expansions in Europe. *Am. Nat.* **128**, 681-706 (1986).
- 506 22 Edmonds, C. A., Lillie, A. S. & Cavalli-Sforza, L. L. Mutations arising in the wave
507 front of an expanding population. *Proc Natl Acad Sci U S A* **101**, 975-979 (2004).
508 [https://doi.org:10.1073/pnas.0308064100](https://doi.org/10.1073/pnas.0308064100)
- 509 23 Klopstein, S., Currat, M. & Excoffier, L. The fate of mutations surfing on the wave
510 of a range expansion. *Mol Biol Evol* **23**, 482-490 (2006).
511 [https://doi.org:10.1093/molbev/msj057](https://doi.org/10.1093/molbev/msj057)
- 512 24 Peischl, S., Dupanloup, I., Bosshard, L. & Excoffier, L. Genetic surfing in human
513 populations: from genes to genomes. *Curr Opin Genet Dev* **41**, 53-61 (2016).
514 [https://doi.org:10.1016/j.gde.2016.08.003](https://doi.org/10.1016/j.gde.2016.08.003)
- 515 25 Travis, J. M. *et al.* Deleterious mutations can surf to high densities on the wave front
516 of an expanding population. *Mol Biol Evol* **24**, 2334-2343 (2007).
517 [https://doi.org:10.1093/molbev/msm167](https://doi.org/10.1093/molbev/msm167)
- 518 26 Austerlitz, F., JungMuller, B., Godelle, B. & Gouyon, P. H. Evolution of coalescence
519 times, genetic diversity and structure during colonization. *Theor Popul Biol* **51**, 148-
520 164 (1997). [https://doi.org:10.1006/tpbi.1997.1302](https://doi.org/10.1006/tpbi.1997.1302)
- 521 27 Li, J. Z. *et al.* Worldwide human relationships inferred from genome-wide patterns of
522 variation. *Science* **319**, 1100-1104 (2008). [https://doi.org:10.1126/science.1153717](https://doi.org/10.1126/science.1153717)
- 523 28 Sousa, V., Peischl, S. & Excoffier, L. Impact of range expansions on current human
524 genomic diversity. *Curr Opin Genet Dev* **29**, 22-30 (2014).
525 [https://doi.org:10.1016/j.gde.2014.07.007](https://doi.org/10.1016/j.gde.2014.07.007)
- 526 29 Currat, M., Ruedi, M., Petit, R. J. & Excoffier, L. The hidden side of invasions:
527 Massive introgression by local genes. *Evolution* **62**, 1908-1920 (2008).
528 [https://doi.org:10.1111/j.1558-5646.2008.00413.x](https://doi.org/10.1111/j.1558-5646.2008.00413.x)
- 529 30 Currat, M. & Excoffier, L. The effect of the Neolithic expansion on European
530 molecular diversity. *Proc Biol Sci* **272**, 679-688 (2005).
531 [https://doi.org:10.1098/rspb.2004.2999](https://doi.org/10.1098/rspb.2004.2999)

- 532 31 Brandt, G. *et al.* Ancient DNA Reveals Key Stages in the Formation of Central
533 European Mitochondrial Genetic Diversity. *Science* **342**, 257-261 (2013).
534 [https://doi.org:10.1126/science.1241844](https://doi.org/10.1126/science.1241844)
- 535 32 Lipson, M. *et al.* Parallel palaeogenomic transects reveal complex genetic history of
536 early European farmers. *Nature* **551**, 368-+ (2017).
537 [https://doi.org:10.1038/nature24476](https://doi.org/10.1038/nature24476)
- 538 33 Silva, N. M., Rio, J., Kreutzer, S., Papageorgopoulou, C. & Currat, M. Bayesian
539 estimation of partial population continuity using ancient DNA and spatially explicit
540 simulations. *Evol Appl* **11**, 1642-1655 (2018). [https://doi.org:10.1111/eva.12655](https://doi.org/10.1111/eva.12655)
- 541 34 Hofmanova, Z. *et al.* Early farmers from across Europe directly descended from
542 Neolithic Aegeans. *Proc Natl Acad Sci U S A* **113**, 6886-6891 (2016).
543 [https://doi.org:10.1073/pnas.1523951113](https://doi.org/10.1073/pnas.1523951113)
- 544 35 Allentoft, M. E. *et al.* Population genomics of Bronze Age Eurasia. *Nature* **522**, 167-
545 172 (2015). [https://doi.org:10.1038/nature14507](https://doi.org/10.1038/nature14507)
- 546 36 Haak, W. *et al.* Massive migration from the steppe was a source for Indo-European
547 languages in Europe. *Nature* **522**, 207-211 (2015).
548 [https://doi.org:10.1038/nature14317](https://doi.org/10.1038/nature14317)
- 549 37 Rio, J., Quilodran, C. S. & Currat, M. Spatially explicit paleogenomic simulations
550 support cohabitation with limited admixture between Bronze Age Central European
551 populations. *Commun Biol* **4**, 1163 (2021). [https://doi.org:10.1038/s42003-021-](https://doi.org/10.1038/s42003-021-02670-5)
552 [02670-5](https://doi.org/10.1038/s42003-021-02670-5)
- 553 38 Chikhi, L., Nichols, R. A., Barbujani, G. & Beaumont, M. A. Y genetic data support
554 the Neolithic demic diffusion model. *Proc Natl Acad Sci U S A* **99**, 11008-11013
555 (2002). [https://doi.org:10.1073/pnas.162158799](https://doi.org/10.1073/pnas.162158799)
- 556 39 Allen Ancient DNA Resource Version 50. (2022).
- 557 40 Burnham, K. P. & Anderson, D. R. *A Practical Information-Theoretic Approach.*
558 *Model Selection and Multimodel Inference.* 2nd edn, (Springer, 2002).
- 559 41 Petr, M., Paabo, S., Kelso, J. & Vernot, B. Limits of long-term selection against
560 Neandertal introgression. *P Natl Acad Sci USA* **116**, 1639-1644 (2019).
561 [https://doi.org:10.1073/pnas.1814338116](https://doi.org/10.1073/pnas.1814338116)
- 562 42 Nielsen, R. *et al.* Tracing the peopling of the world through genomics. *Nature* **541**,
563 302-310 (2017). [https://doi.org:10.1038/nature21347](https://doi.org/10.1038/nature21347)
- 564 43 Juric, I., Aeschbacher, S. & Coop, G. The Strength of Selection against Neanderthal
565 Introgression. *PLoS Genet* **12**, e1006340 (2016).
566 [https://doi.org:10.1371/journal.pgen.1006340](https://doi.org/10.1371/journal.pgen.1006340)
- 567 44 Arenas, M., Francois, O., Currat, M., Ray, N. & Excoffier, L. Influence of admixture
568 and paleolithic range contractions on current European diversity gradients. *Mol Biol*
569 *Evol* **30**, 57-61 (2013). [https://doi.org:10.1093/molbev/mss203](https://doi.org/10.1093/molbev/mss203)
- 570 45 Arenas, M., Ray, N., Currat, M. & Excoffier, L. Consequences of Range Contractions
571 and Range Shifts on Molecular Diversity. *Mol Biol Evol* **29**, 207-218 (2012).
572 [https://doi.org:10.1093/molbev/msr187](https://doi.org/10.1093/molbev/msr187)
- 573 46 Fuller, D. Q., Willcox, G. & Allaby, R. G. Cultivation and domestication had multiple
574 origins: arguments against the core area hypothesis for the origins of agriculture in the
575 Near East. *World Archaeol* **43**, 628-652 (2011).
576 [https://doi.org:10.1080/00438243.2011.624747](https://doi.org/10.1080/00438243.2011.624747)
- 577 47 Bettinger, R. L., Barton, L. & Morgan, C. The Origins of Food Production in North
578 China: A Different Kind of Agricultural Revolution. *Evol Anthropol* **19**, 9-21 (2010).
579 [https://doi.org:10.1002/evan.20236](https://doi.org/10.1002/evan.20236)

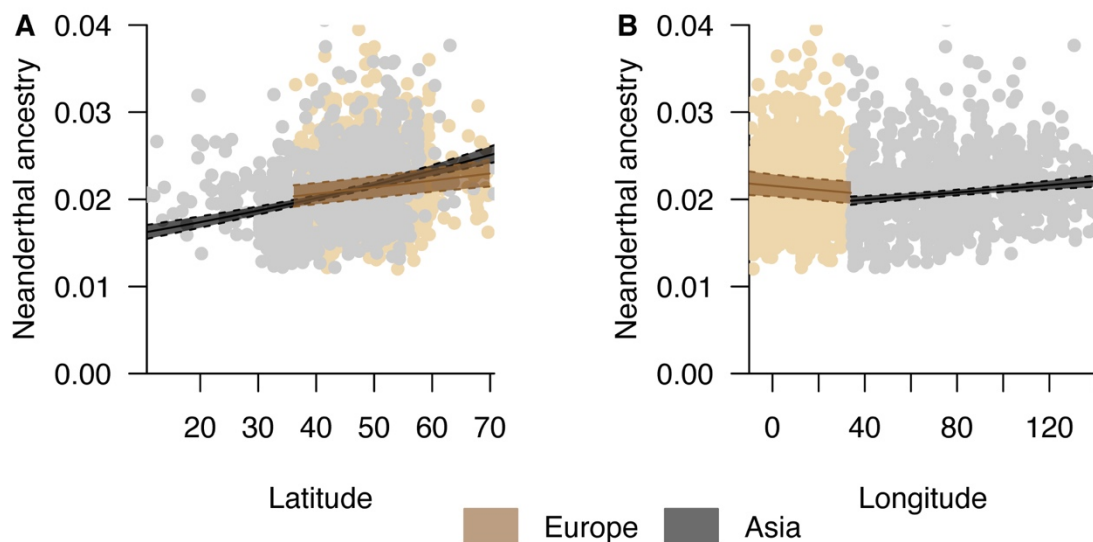
- 580 48 Riehl, S., Zeidi, M. & Conard, N. J. Emergence of Agriculture in the Foothills of the
581 Zagros Mountains of Iran. *Science* **341**, 65-67 (2013).
582 <https://doi.org/10.1126/science.1236743>
- 583 49 Vyas, D. N. & Mulligan, C. J. Analyses of Neanderthal introgression suggest that
584 Levantine and southern Arabian populations have a shared population history.
585 *American Journal of Physical Anthropology* **169**, 227-239 (2019).
586 <https://doi.org/10.1002/ajpa.23818>
- 587 50 Mendez, F. L., Watkins, J. C. & Hammer, M. F. A haplotype at STAT2 Introgressed
588 from neanderthals and serves as a candidate of positive selection in Papua New
589 Guinea. *American journal of human genetics* **91**, 265-274 (2012).
590 <https://doi.org/10.1016/j.ajhg.2012.06.015>
- 591 51 Quach, H. *et al.* Genetic Adaptation and Neandertal Admixture Shaped the Immune
592 System of Human Populations. *Cell* **167**, 643-+ (2016).
593 <https://doi.org/10.1016/j.cell.2016.09.024>
- 594 52 Huerta-Sanchez, E. *et al.* Altitude adaptation in Tibetans caused by introgression of
595 Denisovan-like DNA. *Nature* **512**, 194-+ (2014). <https://doi.org/10.1038/nature13408>
- 596 53 Kerner, G., Patin, E. & Quintana-Murci, L. New insights into human immunity from
597 ancient genomics. *Curr Opin Immunol* **72**, 148-157 (2021).
598 <https://doi.org/10.1016/j.coi.2021.04.006>
- 599 54 Zeberg, H. & Paabo, S. The major genetic risk factor for severe COVID-19 is
600 inherited from Neanderthals. *Nature* **587**, 610-+ (2020).
601 <https://doi.org/10.1038/s41586-020-2818-3>
- 602 55 Nakatsuka, N. *et al.* ContamLD: estimation of ancient nuclear DNA contamination
603 using breakdown of linkage disequilibrium. *Genome Biol* **21**, 199 (2020).
604 <https://doi.org/10.1186/s13059-020-02111-2>
- 605 56 Reich, D., Thangaraj, K., Patterson, N., Price, A. L. & Singh, L. Reconstructing
606 Indian population history. *Nature* **461**, 489-U450 (2009).
607 <https://doi.org/10.1038/nature08365>
- 608 57 Maier, R., Flegontov, P., Flegontova, O., Changmai, P. & Reich, D. Admixtools 2.
609 *bioRxiv* (2022). <<https://github.com/uqrmaie1/admixtools>>.
- 610 58 Zuur, A., Ieno, E. N., Walker, N., Saveliev, A. A. & Smith, G. M. *Mixed Effects*
611 *Models and Extensions in Ecology With R*. (Springer Science & Business Media,
612 2009).
- 613 59 Nakagawa, S., Johnson, P. C. D. & Schielzeth, H. The coefficient of determination R-
614 2 and intra-class correlation coefficient from generalized linear mixed-effects models
615 revisited and expanded. *J R Soc Interface* **14** (2017).
616 <https://doi.org/10.1098/rsif.2017.0213>
- 617



618

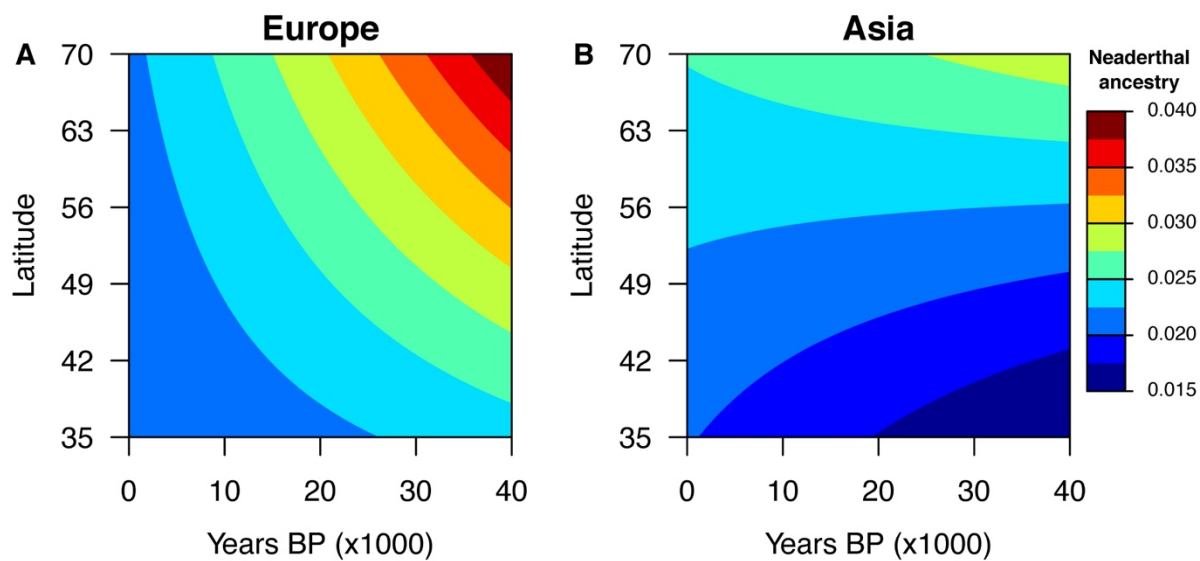
619 **Figure 1:** A) Schematic representation of the expected spatial gradient of introgression from
620 the local taxon into an invasive taxon after a biological invasion with hybridization. B)

621 Distribution of samples in Eurasia used for elucidating spatial gradients of Neanderthal
622 ancestry in modern humans. The coloured dots represent palaeogenomic samples of hunter-
623 gatherers (HG, ~40000–6000 years BP, $n = 129$), early farmers (FA, ~10000–2000 years BP,
624 $n = 679$), other ancient (OT, ~6400–300 years BP, $n = 1726$), and modern (MD, current time,
625 $n = 91$). The dotted ellipse represents the presumed geographic source of the Palaeolithic out
626 of Africa expansion into Eurasia (~50000 years BP), and the dotted circle represents the
627 source of the Neolithic expansion of agricultural populations from the fertile crescent
628 (~11000 years BP). The red triangle represents the longitudinal limit (34°) that, in our study,
629 separates European ($n=1517$) from Asian ($n=1108$) population samples.



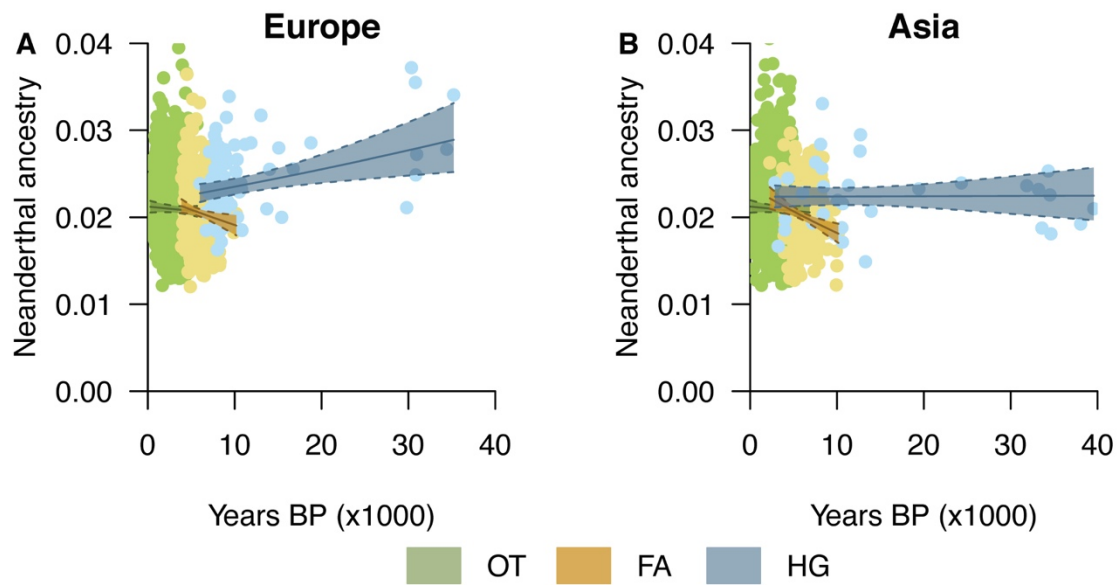
630

631 **Figure 2.** Effects of latitude and longitude on the level of Neanderthal ancestry in both
632 Europe and Asia. The solid and dotted lines represent the estimated values and 95%
633 confidence intervals, respectively. The coloured dots represent the distribution of the full
634 dataset of ancient and modern DNA samples used in the “Full Eurasia” analysis ($n = 2625$).



635

636 **Figure 3.** Influence of latitude and time on the level of Neanderthal ancestry in both Europe
637 and Asia. The analysis considers the full dataset of ancient and modern DNA samples (“Full
638 Eurasia”, $n = 2625$). The y-axis corresponds to the range where both regions (Asia and
639 Europe) have the most data.



640

641

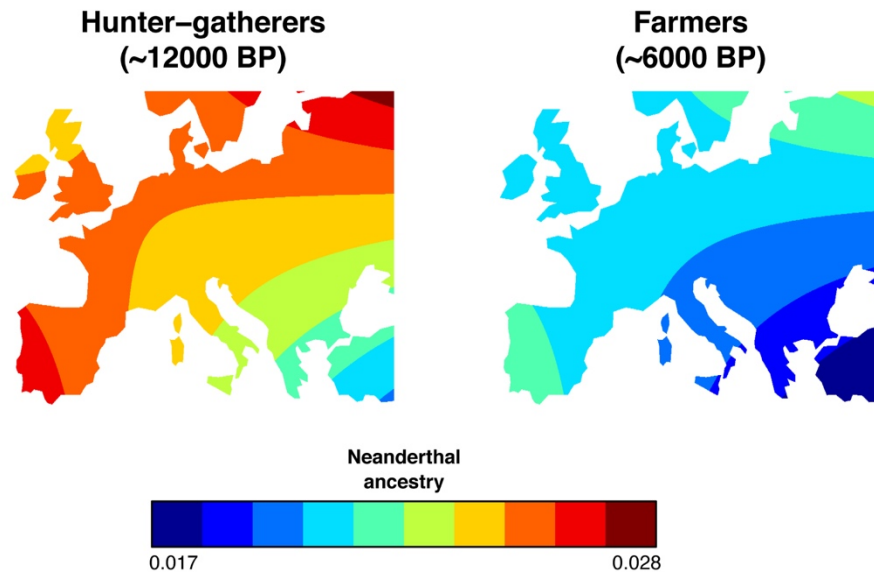
642

643

644

645

Figure 4. Temporal variation in the level of Neanderthal ancestry in different cultural populations of Eurasia. HGs: hunter gatherers, FAs: Neolithic farmers, OTs: other ancient samples. The solid and dotted lines represent the estimated values and 95% confidence intervals, respectively. The coloured dots represent the distribution of ancient DNA samples used in the best “Ancient Eurasia” analysis ($n = 2534$).



646

647 **Figure 5.** Spatial variation on the level of Neanderthal ancestry in European hunter-gatherers

648 (HG) and farmers (FA) projected using the best “Europe” model ($n = 1517$).